Proceedings of the ICBBG2025
2025 International conference on Bio-mediated and Bio-inspired Geotechnics
18-20 May, 2025 | Tempe, Arizona, USA
https://doi.org/10.53243/ICBBG2025-57

Development of a Treatment Strategy Applicable to Field Conditions for the Repair of Vertical Fractures in Concrete Using MICP

Gloria M. Castro[1], Grainne El Mountassir[2], and Rebecca J. Lunn, MBE FREng FRSE FICE [3]

[1] Assistant Professor, Department of Civil Engineering, University of Birmingham, UK (formerly at the University of Strathclyde); email: g.m.castro@bham.ac.uk
[2] Reader, Department of Civil and Environmental Engineering, University of Strathclyde, UK; email: grainne.elmountassir@strath.ac.uk
[3] Distinguished Professor, Department of Civil and Environmental Engineering, University of Strathclyde, UK; email: rebecca.lunn@strath.ac.uk

ABSTRACT

Concrete plays a vital role in infrastructure and is often exposed to harsh conditions. Reducing the permeability of damaged concrete through durable repairs is crucial to prevent further deterioration. This study develops a Microbially Induced Calcite Precipitation (MICP) treatment for field conditions, targeting millimeter-scale, vertical fractures with limited access. Treatment used three injection ports while ultrasonic and representative permeability measurements characterized crack evolution. After treatment, the crack permeability decreased significantly, and the treated block showed a repair tensile strength of 0.5 MPa compared to the original concrete's 2 MPa. SEM-EDS analysis revealed a well-distributed, strongly cemented repair interface. The study demonstrates that MICP can effectively seal vertical fractures, providing a durable, low-permeability repair suitable for field conditions.

INTRODUCTION

Concrete constitutes a large proportion of our built infrastructure, and assets are often exposed to harsh environmental conditions (Fiorio 2005; Xiang et al. 2022). Reducing the permeability of degraded concrete using strong and durable repairs, is key to minimizing further structural deterioration. Current established techniques for concrete repair include cement mortars and epoxy resins (Jumaat et al. 2006; pers. comm. Bam Nuttall UK). These solutions have some limitations: (1) cement mortars have high viscosities, resulting in limited penetration (Miltiadou-Fezans & Tassios 2013); (2) epoxy resins have drastic differences in chemical compositions from concrete, resulting in different thermal expansion behaviors, developing cracks at the interface and delamination (Daneshvar et al. 2021); (3) epoxy resins display sensitivity to humidity and alkaline environments, poor long-term performance, and environmental hazards (Raupach & Wolff 2008; Rudawska et al. 2022).

Microbially Induced Calcite Precipitation MICP emerges as a bio-assisted alternative to enhance porous media (Whiffin 2004; Al Qabany et al. 2012; Lin et al. 2016; Xiao et al. 2023). This technique relies on the metabolic action of microorganisms to promote carbonate crystal precipitation, resulting in a particle-binding and pore-filling cement. Previous studies have recognized the potential use of MICP on concrete and masonry restoration, such as for the

protection of facades (Le Metayer-Levrel et al. 1999), patch repair and infiltration (Wiktor and Jonkers 2016; Qiao et al. 2022), flow-based strategy testing (Tobler et al. 2018; Turner et al. 2023), and limited field grouting testing in small fractures (Zhang et al. 2013). These studies have contributed immensely to the development of MICP as a repair biotechnology; nevertheless, the methodologies proposed for MICP repair are not applicable to most field conditions (i.e. limited access, vertical and millimeter-scale fractures). Additionally, monitoring and assessment of the repair was often limited to visual observations.

This study aims to develop a MICP treatment strategy applicable to field conditions, considering vertical fractures with limited access and millimeter-scale apertures. Experimental studies use a "transparent fracture" made of acrylic plates for the development of the treatment methodology. The treatment implementation uses a 25 cm side concrete cube with a vertical fracture of about 7mm aperture and limited access to the front face. Repaired block was assessed by ultrasound testing, representative permeability measurements and tensile strength testing. Post-mortem analyses include repair distribution by image analysis, and SEM-EDS characterizations.

TRANSPARENT "FRACTURE": METHODOLOGY DEVELOPMENT

Previous studies have successfully repaired concrete and masonry by injecting multiple MICP treatment cycles, even considering highly tortuous and rough fractures (Tobler et al. 2018; Turner et al. 2023). Nevertheless, the methodology proposed displayed a consistent hydraulic aperture reduction of about 5 μm per MICP cycle, limiting its application to micrometer-scale fractures due to time constraints under field commercial applications. To overcome this issue, we propose to inject a filler as part of the first treatment cycle, ensuring a fast and strong repair. To validate the proposed strategy, we started by using a transparent fracture in this section.

Exploration of Injection Methodology

Transparent "Fracture"

The limited accessibility to the fracture depth and hence the uncertainty on the success of the repair is a key challenge when developing a MICP methodology applicable to repair concrete under field conditions.

This study starts by using two transparent "fractures" formed by Plexiglas plates of 30 cm side separated by rubber spacers that control the fracture aperture at 1 cm (Figure 1). In the first scenario, we assume that the fracture is developing and has not reached the other side of the concrete volume ("One-side open fracture" Figure 1a). The second scenario considers a fracture that propagated all the way to the back of the element, and we have access to the two ends ("Two-side open fracture" Figure 1b). This experimental setup allows visual access to the distribution of the filler and treatment fluids inside the fracture to define a treatment strategy.

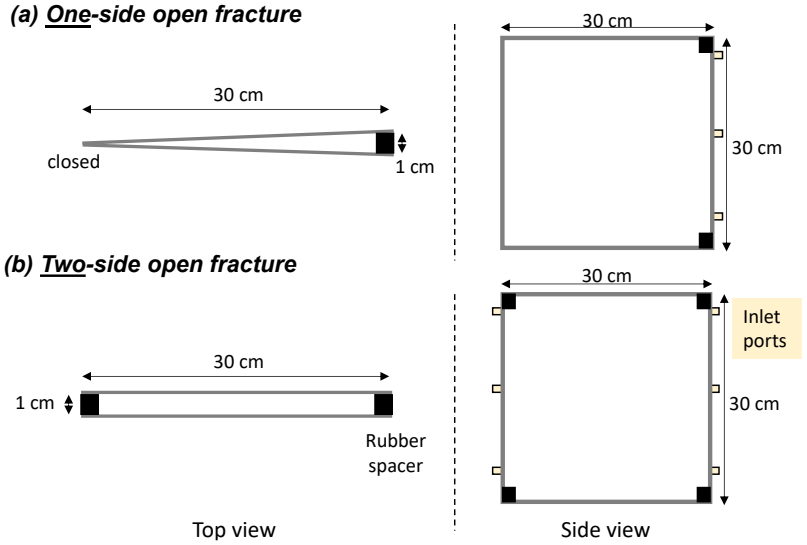

Fig 1. Transparent "fracture" experimental setup. (a) One-side and (b) two-side open fracture

Acrylic plates were joined by a latex paste which formed a solid membrane after 10 hours in contact with oxygen (from Restorative Techniques UK). The accessible sides of the fractures contained inserted plastic luer to hose barbs used as tubing inlets and the bottom boundary had a fine mesh instead of the latex membrane to simulate a boundary that is opened to fluid flow but closed to filler material flow.

Filler Injection

The volume fraction φ, Reynolds number R_e and the ratio between particle diameter to tube diameter d_{part}/d_{tub} affect the flow of large particles through a pipe (Revstedt et al. 2023). The following items were considered when designing the filler injection strategy:

- *Inlet size*: The diameter of the inlet will depend on the size of the fracture. In this case, a 1cm fracture allowed us to insert a tubing of maximum 1.5 mm internal diameter.
- *Minimum number of injections*: We aimed to get the most filler in with the least number of injections. Therefore, we used a high volume fraction φ=25% considering a moderate R_e number, and using tap water as the liquid solution (Revstedt et al. 2023).
- *Flowability of grains*: Sand was chosen as the filler material to ensure enough pore space for bacteria mobility (Mitchell & Santamarina 2005). Particle size was defined based on flowability at the defined volume fraction and considering the maximum tube diameter (d_{part}/d_{tub} =14%, Table 1). The filler material consisted of a quarzitic poorly graded sand with d_{50}=0.21 mm.
- *Practical and inexpensive injection*: We used widely available 60 ml syringes with the tip cut to fit a 1.5 mm I.D. tubing.

Table 1. Flowability of the filler material at variable particle to tube diameter ratios d_{part}/d_{tub}

d_{part}/d_{tub} [%]	11	14	26
Flow	yes	yes	clogged

Filler Injection Procedure

(1) Prepared the filler material at the target volume fraction and poured it into the prepared 60 ml syringe with the tubing attached to the outlet of the syringe.
(2) Inserted the tubing to the back of the fracture through the bottom inlet port.

(3) Shaked the material inside the syringe and injected it into the fracture using the syringe plunger.
(4) Repeated the procedure using the following inlet port above.

Filler distribution within the fracture

Figure 2a and 2b shows photographic images of the one-side open fracture before and after the injection of the filler (Fig. 1a). We obtained an overall uniform filler distribution along the fracture even as the fracture opening reduces towards the left side (where it is closed). The filler material did not reach the top left corner which may cause a weak area within the repair (Fig. 2b).

Figure 2d and 2e displays images of the two-side open fracture before and after filler injection (Fig. 1b). We only used the right-side injection ports for filler injection to provide less disturbance to the filler material. In this case, the injected sand reached all the fracture space, as a more uniform aperture facilitates the distribution of the material (Fig. 2e).

Treatment Fluids: Injection Flow Rate

Treatment fluids injection used disposable hypodermic needles of 21G, 1.5" (O.D. of 0.82 mm and 38.1 mm length). The needles were inserted through the solid latex membrane near the filler injection ports. All the needles on each injection side (3 inlets) were connected to one peristaltic pump. This is in case one of the needles clogged due to bio-precipitates while fluids were being injected unsupervised. Therefore, to define the flow rate, we assume the worst-case scenario where two needles are clogged and only one inlet is carrying all the fluid.

Considering a sand with saturated unit weight γ^{sat}=18 kN/m^3, the critical hydraulic gradient i_{crit}=0.83. The area that will be most prompt to boiling will be the soil just around the needle tip (A~1cm^2), and assuming a sand hydraulic conductivity k=0.05 m/s (based on the d_{50}=0.21; Ren & Santamarina 2018; Chandel & Vijay 2022), we can calculate a maximum flow rate of Q=2.5 ml/min to prevent boiling. As the MICP treatment takes place, the hydraulic conductivity of the material will decrease, but the bio-mediated precipitates will bind particles together reducing the susceptibility to boiling.

A cementing solution consisting of 1M $CaCl_2$ and urea was dyed with laboratory graded fluorescein and injected through the three ports in the two filled fractures at a total flow rate Q=2.5 ml/min (distributed along the three ports) to assess the reach of the solution along the fracture space (Fig. 2c and 2f). The dyed cementing solution had limited reach towards the closed end of the variable thickness fracture (Fig. 2c). Nevertheless, as MICP cycles progress, the uncemented path may become a flow path connecting the top of the fracture to the outlet at the bottom. Injection of the dyed cementing solution on the homogeneous aperture fracture took place from the two accessible sides (6 ports). The cementing solution showed a homogeneous distribution along the filled fracture (Fig. 2f).

MICP Treatment Trial

After designing a methodology that ensured a well distributed filler and cementing solution along both transparent fracture setups, we proceeded to treat the transparent fracture with homogeneous aperture (Fig. 1b).

Materials

This study used a quarzitic, poorly graded *sand* with a mean particle diameter d_{50}=0.21 mm. The *cementing solution C.S.* was composed of 1M urea and calcium chloride (commercial grade). *Bacterial solution* consisted of S. Pasteurii cells suspended in growth media, prepared from cryopreserved stock, with an average optical density OD_{600}= 1 (details of the growth procedure in Turner et al. 2023).

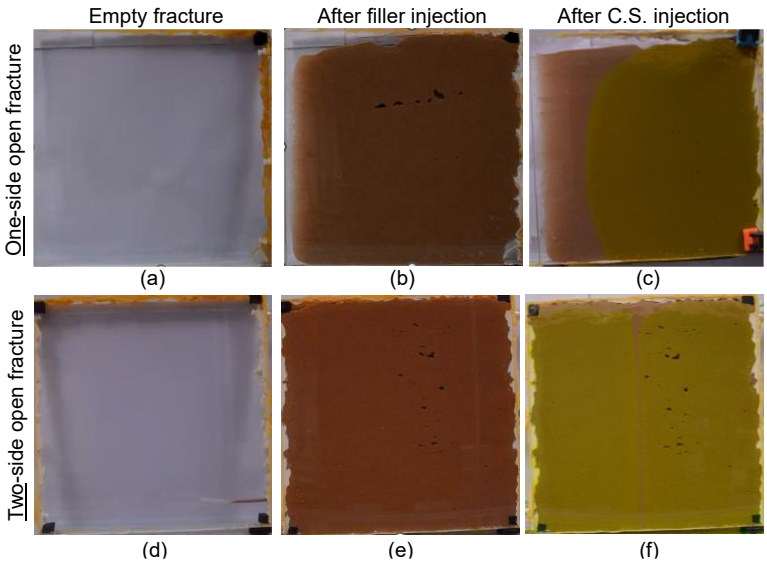

Fig 2. Filler and cementing solution injection in the one-side open fracture (a to c) and in the two-side open fracture (d to f).

Procedure

First cycle

(1) Filler injection: The filler composed of sand and bacteria solution, prepared at a volume fraction φ=25% was injected starting from the bottom port and finishing at the top (as much material as possible). After injection, the ports were closed using parafilm.

(2) Static period: We allowed one hour of static period (no injection flow), to enhance bacterial attachment to solid surfaces.

(3) Cementing solution injection: Three needles were inserted on each side near the filler injection ports. The needles were then connected to plastic tubes and to one peristatic pump on each inlet side (one pump for each three inlets). A volume of 250 ml of cementing solution was injected from each side using the six ports at a flow rate of Q = 0.25 ml/min (500 ml in total= 0.56 initial pore volume PV). A lower flow rate was chosen for the cementing solution to avoid shearing the bacteria cells off the solid grain surfaces.

Following cycles

(1) Static period (1h).

(2) Injection setup clearing: The needles were extracted from the soil, and tubing and needles were flushed with a 50 mM NaCl solution to remove residuals. Needles were replaced if showed signs of clogging.

(3) Bacteria solution injection: The needles were placed back into the same positions and 200 ml of bacteria solution was injected on each fracture side using the six injection ports, when possible, at 2.5 ml/min (400 ml in total).

(4) Static period (1h) followed by setup cleaning (step 2).

(5) Cementing solution injection (repeat step 3 of the first cycle).

The procedure above was applied to the two sides open fracture during six MICP cycles. The treatment was stopped due to increased breakage on the latex membrane as overpressure developed during fluid injection. After treatment cycles 1 to 4 photographic images were taken on the side of the fracture. During cycles 5 and 6 fluorescein was added to the cementing solution to observe the invasion of the cementing and bacterial solution (undyed) into the treated porous medium.

Permeability measurement

After the last cycle, the treated fracture was set horizontally, and additional clamps and latex paste were added to hold the acrylic plates together. One syringe was inserted in the middle position at one end, and an outlet was opened on the latex at the opposite side. A 50 mM NaCl solution was injected at controlled flow rates and the pressure built at the inlet port was measured by a pressure transducer.

Calcium carbonate content

The calcium carbonate content C_C [%] of the treated soil was measured by acid dissolution. This procedure uses a 4% hydrochloric acid solution to dissolve the carbonate contained in the soil. The calcium carbonate content is calculated with the difference in weight of the material before and after dissolution.

Results and Analyses

Figure 3 shows calcite localization in black based on lateral pictures taken after each of the first four cycles (thresholded using ImageJ). The blue arrows show the ports used for injection on each cycle. Treatment fluid injection during cycles 2-4 were restricted to the top ports to enhance the use of the fluids with higher time within the sediment. In general, precipitates localization occurs near the fracture boundaries with enhanced precipitation at the top of the fracture. This localization hints to the rapid use of the cementing solution near the injection ports.

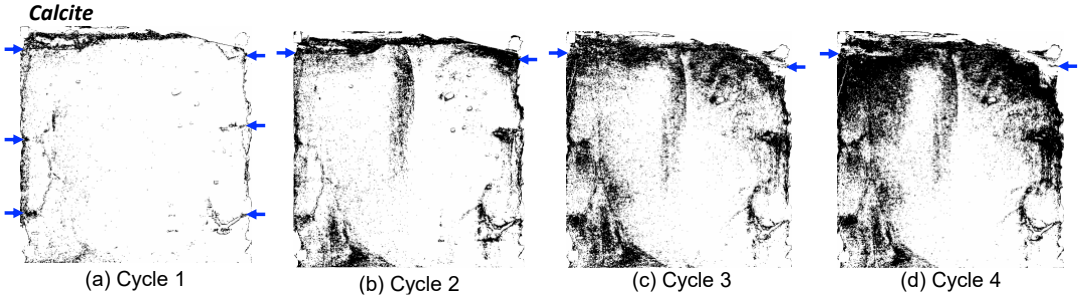

Fig 3. Calcite precipitates localization after the first four MICP treatment cycles. Blue arrows display the ports used for injection on each cycle. (a) Cycle 1, (b) cycle 2, (c) cycle 3, (d) cycle 4.

Cycles 5 and 6 used only the middle ports due to restricted flow through the top (latex breakage suggesting high pressures). Snapshots of the invasion of dyed cementing and undyed bacteria solutions into the treated porous media showed that even on the 6th cycle, the permeability of the porous media was relatively homogenous within the treated fracture, as no preferential paths were observed (Fig. 4). The overall permeability of the treated fracture was measured as 1.68 x10^{-15} m^2 resulting in a reduction of about nine orders of magnitude from the initial opened fracture (8.3 x10^{-6} m^2 based on the cubic law, k [m^2] = a^2/12; where a=1x10^{-2}m).

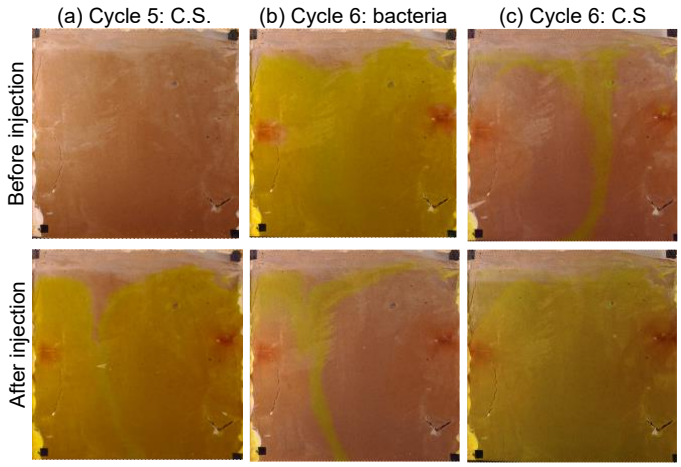

Fig 4. Treatment fluids injection in cycles 5 and 6. (a) Cementing solution injection in cycle 5; (b) Bacteria solution injection in cycle 6; (c) cementing solution injection during cycle 6.

After the final permeability measurement, the repair was extracted from the acrylic plates and divided into a grid of 5x5 squares of 6 cm side. Carbonate content C_C was then measured on every other square, displaying an overall well-distributed precipitation pattern (Fig. 5). Nevertheless, low C_C values near the middle-bottom injection ports suggest that the injection through the bottom ports should not be avoided as treatment fluids were rapidly used near the injection ports used (middle and top), resulting in reduced resources available to the bottom area.

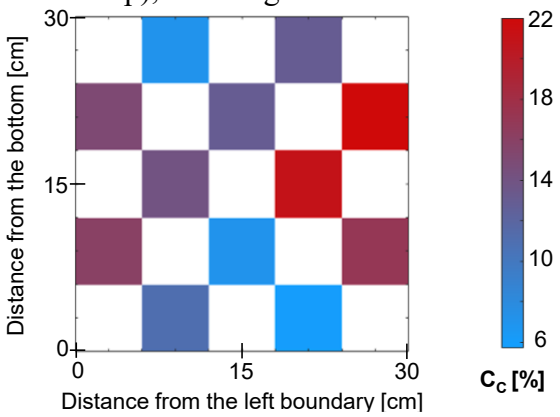

Fig 5. Carbonate content along the repaired fracture after 6 MICP cycles.

METHODOLOGY APPLICATION: CONCRETE CUBE WITH FIELD-LIKE CONDITIONS

This section presents the application of the proposed methodology to repair a 25 cm side concrete cube with a tortuous and heterogeneous vertical fracture considering field-like conditions.

Sample Preparation

Block Setup

A 25 cm side concrete block was cast in the laboratory and tested in tension to generate a realistic vertical fracture (tortuous and heterogeneous; Fig. 6a). The splitting tensile strength procedure was followed obtaining a tensile strength of 2 MPa (BS EN 12390-6 2009). The two sides of the split cube were opened and quarzitic gravel with particle sizes between 4 – to – 4.75 mm randomly allocated to enlarge the fracture aperture, resulting in an average fracture aperture of 7 mm to

represent observed field fracture apertures (Fig. 6b). The two sides of the block were then joined, and latex paste was applied on all fracture faces to obtain control boundary conditions necessary for initial measurements.

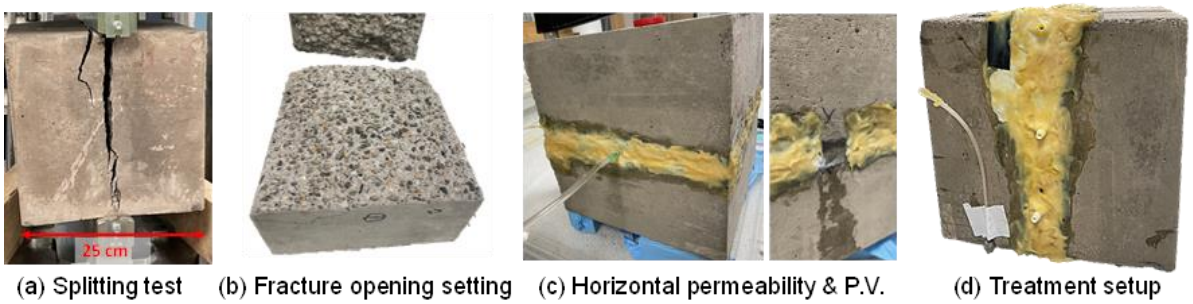

Fig. 6. Concrete Block Repair: Preparation. (a) Splitting test for the creation of a vertical fracture; (b) fracture opening setting; (c) horizontal permeability and pore volume measurements; (d) MICP treatment setup.

Initial Pore Volume and Permeability Measurements

A hypodermic needle was inserted in the middle of one of the sides of the cube and an opening was cut on the opposite side (after latex curing, Fig. 6c). The fracture was then injected at Q =1 ml/min with a 50 mM NaCl solution through the needle and the injection pressure was monitored. When the injection pressure and the volume of fluid collected at the outlet were constant, the fluid was dyed, and samples of the outlet were taken to monitor the breakthrough of the dyed fluid to obtain an estimation of the fracture initial pore volume. After the pore volume measurement, the fracture was left overnight with a constant flow of undyed 50 mM NaCl at Q =1 ml/min. The following day, the injection flow rate was changed to Q =2 and 2.5 ml/min and the injection pressure was allowed to reach equilibrium in each case to measure the initial fracture permeability. Afterwards, the latex membrane was removed at the bottom boundary and a mesh was added in place to allow fluid flow. Furthermore, the cube was clamped and turned to set the fracture vertically, and three injection ports were inserted through the front face (Fig 6d). This assumes similar conditions as in the field, with access only through the front face and free fluid flow though the bottom of the fracture.

Materials

A well-graded calcium carbonate sand with a mean particle size d_{50}=0.18 mm quarried from pure limestone deposits in Derbyshire (Longcliffe) was used as a filler in place of the quarzitic sand. Calcium carbonate sand provides positively charged termination sides which may enhance negatively charged bacteria cells adhesion. Additionally, a better gradation aims to provide a distribution of particle sizes that will account for the tortuosity and differences in fracture aperture along the real fracture. Treatment solutions were as described above in the transparent fractures section.

Monitoring

Representative Permeability Measurements

Before every MICP cycle, a constant flow of 50 mM NaCl was injected through a needle from the top-front face of the block, and the injection pressure was monitored. Considering the bottom of the block as an open boundary, we calculated the permeability of the repair assuming that the complete filler was saturated and there was seepage through all the porous media inside. We call this measurement a representative permeability as we cannot ensure that the medium is uniform

and fully saturated when measurements are taking place, yet it provides feedback of the progress of the MICP treatment cycles.

Ultrasonic Measurements

A pundit equipment was used at the end of the MICP treatment to assess the homogeneity of the repair along the fracture depth (Pundit-200 Proceq, with 54 kHz transducers connected). The transmitter and receiver transducers were set in contact with the concrete block across the repaired fracture at two distances (b_1=10.35 cm and b_2=20.7 cm) at four locations along the fracture depth (Fig. 7a).

MICP Treatment

The MICP treatment strategy applied to the concrete block follows the procedures used on the transparent fracture with detailed quantities specified on Table 2. Before and after the MICP treatment, pore volume and horizontal permeability measurements were performed. Vertical permeability measurements were taken after every MICP cycle.

Table 2. MICP treatment strategy applied to the concrete block

	MICP treatment step description
Cycle 1	Carbonate sand + 0.35 PV open fracture of bacteria solution (recirculated if needed)
	1 hour static
	2 PV (estimated PV after sediment injection) C.S. injected overnight (~1.9 ml/min)
	1 hour static
Cycles 2 to 8	0.35 PV (open fracture) bacteria injected at 2.5 ml/min
	1 hour static
	2 PV (estimated PV after sediment injection) C.S. injected overnight (~1.9 ml/min)
	1 hour static

RESULTS AND ANALYSES: REPAIRED BLOCK CHARACTERISTICS

Wave Transmission

Arrival times at measurements taken further from the latex membrane (b_2 in Fig. 7a and b), display a consistent enhanced wave transmission (i.e. reduced arrival time) along the fracture depth in comparison to measurements of an empty fracture prepared following the same procedure but without the MICP treatment. Measurements taken too closed to the latex membrane did not show significant variations (top values of b_1 in Fig. 7a).

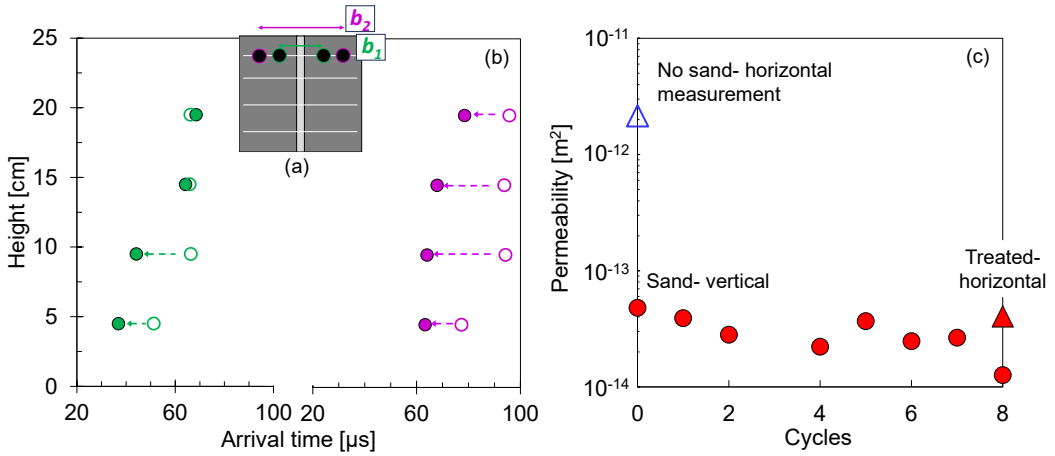

Fig. 7. Transmission properties after MICP treatments. (a) p-wave arrival time along repaired fracture depth. Open symbols display values for an open fracture joint by a latex membrane and filled symbols display measurements after 8 MICP cycles; (b) fluid permeability evolution during the treatment process. Triangles display horizontal measurements and circles vertical.

Permeability and Pore Volume Reduction

Horizontal and vertical permeability measurements display a permeability reduction of about two orders of magnitude (Fig. 7b). Most of the reduction in permeability is given by the injection of the filler (carbonate sand + bacteria), and additional drop in permeability results as bio-precipitates bind the sediment inside the concrete fracture. Additionally, the pore volume of the fracture was reduced by 84% (1150 ml before treatment and 190 ml after). Both reduction in permeability and pore volume are key in the decrease in concrete degradation as it diminishes the ingress and retention of damaging substances.

Mechanical Strength

A tensile splitting test (BS EN 12390-6 2009) was performed on the repaired concrete block with the repaired fracture aligned with the supports to concentrate the tensile stresses in the repair. Nevertheless, the specimen displayed failure through the original concrete in some locations (see red and blue squares in Fig. 8a). The final strength of the recovered block was 0.5MPa, which compares well with the initial concrete strength of 2MPa. The broken repair displayed minimal loose sand, remaining as solid broken pieces.

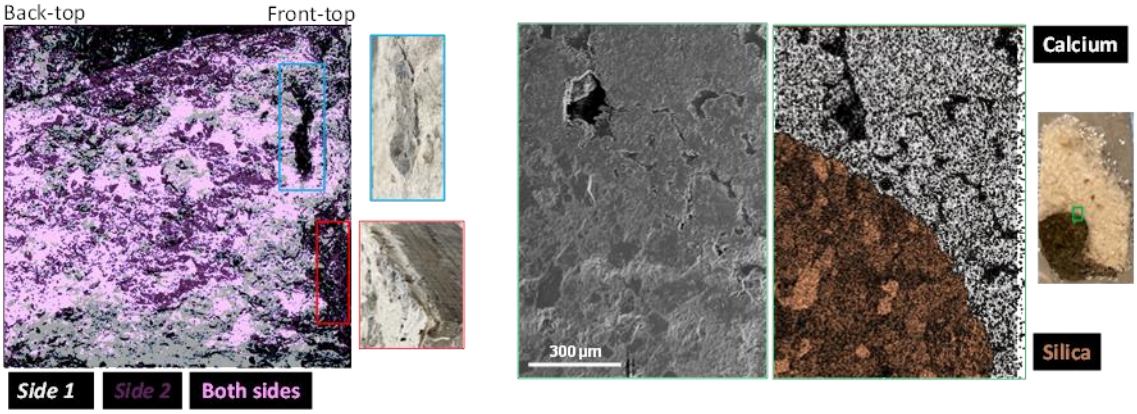

Fig. 8. Characterization of failed specimen. (a) Overlapped thresholded images of the fracture surfaces after failure highlighting repair localization; (b) SEM image of interface between the

original concrete and the repair; (c) EDS map of the region in (a), highlighting the localization of silica-and-calcium-containing compounds

Repair Distribution

After failure, both sides of the fracture were photographed, and the repair was thresholded (Fig. 8a, repair in *Side 1* in white, repair in *Side 2* in dark purple and repair in both sides in light pink). The repair showed overall a good distribution along the fracture with limited reach towards the fracture back-top area. Particularly, areas shown in squares blue and red display section where the specimen failed through the original concrete showing the intact repair in the associated picture.

Repair-Concrete Interface

Figure 8b and 8c show SEM-EDS images of the interface between an aggregate from the original concrete and the repair. The specimen was prepared from a core drilled through the failed fracture, obtaining the intact interface between the repair and concrete. The SEM image displays a smooth transition that is consistent with the mechanical results, where the specimen displayed failure either within the repair or within the concrete but not at the interface, showing excellent adhesion properties of MICP.

CONCLUSIONS

This study proposes a detailed methodology for the use of MICP as a repair technique for fractured concrete under field conditions. The process identified key considerations when defining the treatment methodology: (1) fracture aperture and tortuosity to define the needed filler and tubing for filler injection, (2) filler particle size to define critical injection rates. The proposed methodology was applied to a concrete block with a ~7mm tortuous fracture, achieving a significant reduction in permeability and tensile strength recovery. Also, micro-scale analyses showed the continuous and well attached repair-concrete bond. The use of representative permeability measurements and ultrasonic equipment provide insights into the evolution of the repair treatment.

Further studies will focus on assessing the repeatability of the repair results and will expand on the use of ultrasonic monitoring after each MICP treatment cycle.

REFERENCES

Al Qabany, A., Soga, K., & Santamarina, C. (2012). “Factors affecting efficiency of microbially induced calcite precipitation”. *Journal of Geotechnical and Geoenvironmental Engineering*, *138*(8), 992-1001.

BS EN 12390-6 (2009) “Testing hardened concrete: Part 6: Tensile splitting strength of test specimens” (London: British Standard) pp 1-14

Chandel, A., & Shankar, V. (2022). “Assessment of hydraulic conductivity of porous media using empirical relationships”. *Modeling of Sediment Transport*. *IntechOpen*.

Daneshvar, D., Deix, K., & Robisson, A. (2021). “Effect of casting and curing temperature on the interfacial bond strength of epoxy bonded concretes”. *Construction and Building Materials*, 307, 124328.

Fiorio, B. (2005). “Wear characterisation and degradation mechanisms of a concrete surface under ice friction”. *Construction and Building Materials*, 19(5),366-375.

Jumaat, M. Z., Kabir, M. H., & Obaydullah, M. (2006). "A review of the repair of reinforced concrete beams". *Journal of Applied Science Research*, 2(6), 317-326.

Le Metayer-Levrel, G., Castanier, S., Orial, G., Loubière, J. F., & Perthuisot, J. P. (1999). "Applications of bacterial carbonatogenesis to the protection and regeneration of limestones in buildings and historic patrimony". *Sedimentary geology*, 126(1-4), 25-34.

Lin, H., Suleiman, M. T., Brown, D. G., & Kavazanjian Jr, E. (2016). "Mechanical behavior of sands treated by microbially induced carbonate precipitation". *Journal of Geotechnical and Geoenvironmental Engineering*, *142*(2), 04015066.

Miltiadou-Fezans, A., & Tassios, T. P. (2013). "Penetrability of hydraulic grouts". *Materials and Structures*, 46, 1653-1671.

Mitchell, J. K., & Santamarina, J. C. (2005). "Biological considerations in geotechnical engineering". *Journal of geotechnical and geoenvironmental engineering*, *131*(10), 1222-1233.

Qiao, J., He, J., Xu, X., Guo, H., & Cheng, X. (2022). "Experimental study on the influencing factors of repairing white marble beam by MICP". *Geotechnical Engineering for the Preservation of Monuments and Historic Sites III* (pp. 379-388). CRC Press.

Raupach, M., & Wolff, L. (2008). "Durability of adhesion of epoxy coatings on concrete; causes of delamination and blistering". *Concrete Repair, Rehabilitation and Retrofitting II* (pp. 355-356). CRC Press.

Ren, X. W., & Santamarina, J. C. (2018). "The hydraulic conductivity of sediments: A pore size perspective". *Engineering Geology*, 233, 48-54.

Revstedt, J., Innings, F., & Arlov, D. (2023). "Effects of large particles in pipe flow at low and moderate Reynolds numbers". *Chemical Engineering & Technology*, *46*(7),1387-1396.

Rudawska, A., Sarna-Boś, K., Rudawska, A., Olewnik-Kruszkowska, E., & Frigione, M. (2022). "Biological effects and toxicity of compounds based on cured epoxy resins". *Polymers*, 14(22), 4915.

Turner, R., Castro, G. M., Minto, J., El Mountassir, G., & Lunn, R. J. (2023). "Treatment of fractured concrete via microbially induced carbonate precipitation: From micro-scale characteristics to macro-scale behaviour". *Construction and Building Materials*, *384*, 131467.

Whiffin, V. S. (2004). "Microbial CaCO3 precipitation for the production of biocement". Doctoral dissertation, Murdoch University.

Wiktor, V., & Jonkers, H. M. (2016). "Bacteria-based concrete: from concept to market". *Smart Materials and Structures*, 25(8), 084006.

Xiang, J., Liu, H., Lu, H., & Gui, F. (2022). "Degradation mechanism and numerical simulation of pervious concrete under salt freezing-thawing cycle". *Materials*, 15(9), 3054.

Xiao, G., Zhang, J., & Cheng, X. (2023). "Review on the Application of Biogeotechnology in the Restoration of Masonry Structures". *Geomicrobiology Journal*, 40(8-10), 719-732.

Zhang, Y., Guo, H. X., Cheng, X. H., & Li, M. (2013). "Field experiment of microbial induced carbonate precipitation technology in leakage treatment of a basement". *Industrial Construction*, *43*(12), 138-143.